

Fluxional processes and structural characterization of $\mu_3\text{-}\eta^2,\eta^2,\eta^2\text{-C}_{60}$ triosmium cluster complexes, $\text{Os}_3(\text{CO})_{9-n}(\text{PMe}_3)_n(\mu_3\text{-}\eta^2,\eta^2,\eta^2\text{-C}_{60})$ ($n = 1, 2, 3$)

Hyunjoon Song ^a, Kwangyeol Lee ^a, Joon T. Park ^{a,*}, Hong Young Chang ^b, Moon-Gun Choi ^b

^a Department of Chemistry and Center for Molecular Science, Korea Advanced Institute of Science and Technology, Taejeon, 305-701, South Korea

^b Department of Chemistry, Yonsei University, Seoul, 120-749, South Korea

Received 7 September 1999; received in revised form 20 November 1999

Abstract

The title complex, $\text{Os}_3(\text{CO})_6(\text{PMe}_3)_3(\mu_3\text{-}\eta^2,\eta^2,\eta^2\text{-C}_{60})$ (**3**), has been prepared by decarbonylation of $\text{Os}_3(\text{CO})_9(\mu_3\text{-}\eta^2,\eta^2,\eta^2\text{-C}_{60})$ with three equivalents of Me_3NO in the presence of excess PMe_3 ligand. The solid-state structures of $\text{Os}_3(\text{CO})_7(\text{PMe}_3)_2(\mu_3\text{-}\eta^2,\eta^2,\eta^2\text{-C}_{60})$ (**2**) and **3** have been determined by single-crystal X-ray diffraction studies. Compound **2** has two inequivalent equatorial phosphine ligands on adjacent osmium atoms and compound **3**, with a distorted C_3 symmetry, has one equivalent equatorial phosphine ligand on each osmium center. The fluxional processes of $\text{Os}_3(\text{CO})_8(\text{PMe}_3)(\mu_3\text{-}\eta^2,\eta^2,\eta^2\text{-C}_{60})$ (**1**), **2**, and **3** have been examined by variable-temperature ^{13}C - and ^{31}P -NMR studies. Only one isomer exists in solution and a restricted ligand rotation on each phosphine-substituted osmium center appears to occur for all three compounds, **1–3**. Activation barriers for the carbonyl exchange process increase with increasing phosphine substitution, presumably, due to the steric effect of the phosphine ligands. © 2000 Elsevier Science S.A. All rights reserved.

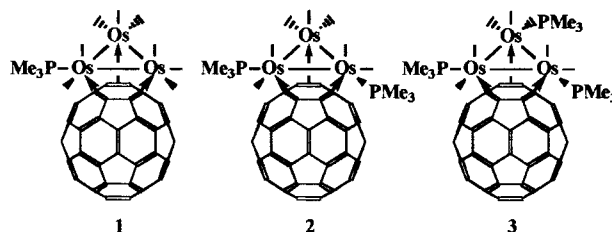
Keywords: Metallofullerene; Triosmium carbonyl cluster; Crystal structure; Phosphine; Fluxional processes

1. Introduction

Addition reactions to the double bond at the 6:6 ring junction of electronegative alkene-like C_{60} are a prominent feature of exohedral organometallic fullerene chemistry [1]. While numerous reports on metal coordinated C_{60} complexes have revealed η^2 - or $\mu\text{-}\eta^2,\eta^2\text{-C}_{60}$ bonding modes for mono- or dinuclear metal complexes [2–5], the face capping $\mu_3\text{-}\eta^2,\eta^2,\eta^2\text{-C}_{60}$ is the dominant form of C_{60} interaction with multinuclear cluster frameworks. Cluster frameworks that can form stable $\mu_3\text{-}\eta^2,\eta^2,\eta^2\text{-C}_{60}$ complexes include Os_3 [5,6], Ru_3 [7], Ru_5C , Ru_6C , and PtRu_5C [8] clusters.

Most of the reports on the exohedral C_{60} –metal complexes have been focused on their synthesis and structural characterization, but little has been reported on the reactivity studies of these compounds. We have shown

previously that triosmium carbonyl C_{60} compounds can be activated by Me_3NO in the presence of external ligands to provide acetonitrile or phosphine derivatives [4–6]. As an extension of our previous work, we have prepared a tris(trimethylphosphine) derivative $\text{Os}_3(\text{CO})_6(\text{PMe}_3)_3(\mu_3\text{-}\eta^2,\eta^2,\eta^2\text{-C}_{60})$ (**3**) by an analogous method. In this paper, we report the synthesis and the characterization of **3**, and the structural determination of $\text{Os}_3(\text{CO})_7(\text{PMe}_3)_2(\mu_3\text{-}\eta^2,\eta^2,\eta^2\text{-C}_{60})$ (**2**) and **3**, together with a systematic investigation on the fluxional processes of $\text{Os}_3(\text{CO})_8(\text{PMe}_3)(\mu_3\text{-}\eta^2,\eta^2,\eta^2\text{-C}_{60})$ (**1**), **2** and **3** by variable temperature (VT) ^{13}C - and ^{31}P -NMR studies.



* Corresponding author. Fax: +82-42-8692810.

E-mail address: jtpark@sorak.kaist.ac.kr (J.T. Park)

2. Results and discussion

2.1. Synthesis and characterization of **3**

The synthesis and characterization of compounds **1** and **2** have been reported in our earlier accounts [5,6]. Complex **3**, $\text{Os}_3(\text{CO})_6(\text{PMe}_3)_3(\mu_3\text{-}\eta^2, \eta^2, \eta^2\text{-C}_{60})$, has been prepared in 55% yield together with **2** (9%) as a minor product, by initial decarbonylation of $\text{Os}_3(\text{CO})_9(\mu_3\text{-}\eta^2, \eta^2, \eta^2\text{-C}_{60})$ with three equivalents of $\text{Me}_3\text{NO-CH}_3\text{CN}$ at 0°C in the presence of excess PMe_3 and subsequent heating at 70°C for 1 h. Formulation of **3** is established by elemental analysis and positive-ion FAB mass spectroscopy. The molecular ion $[\text{M}^+]$ isotope multiple in the mass spectrum of **3** matches the calculated pattern perfectly: the highest peaks in the M^+ multiplet (m/z , found, Anal. Calc.) are (1688, 1688). The carbonyl bands in the IR spectrum of **3** are shifted to the lower energy region by ca. 40 cm^{-1} than those of **2** [6], reflecting a significant donor effect of the PMe_3 ligand. Compound **3** is soluble in common solvents such as dichloromethane, carbon disulfide, and chlorinated benzenes to form a brown solution. It is stable in refluxing chlorobenzene over 1 day, and does

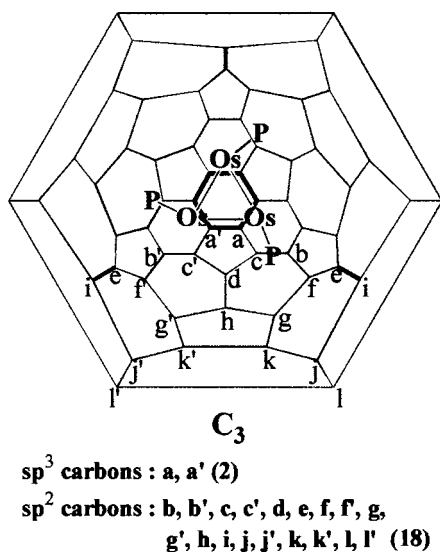
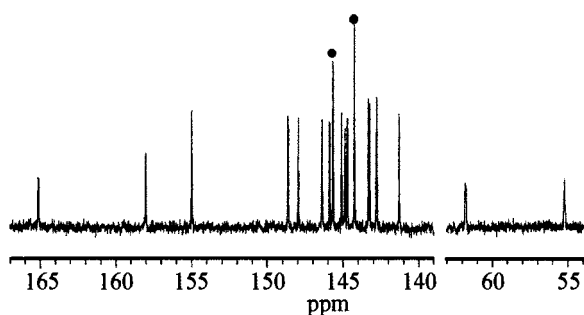


Fig. 1. ^{13}C -NMR spectrum (100 MHz, $o\text{-C}_6\text{H}_4\text{Cl}_2\text{-C}_7\text{D}_8$, C_{60} region) of **3** and an analysis of the different carbon types in C_{60} . Resonances with an intensity of two are labeled as ●.

not undergo any further reaction either by treatment with Me_3NO or under prolonged irradiation of ultraviolet light.

The $^{31}\text{P}\{^1\text{H}\}$ -NMR spectrum of **3** shows a singlet at $\delta -54.3$, indicating that three phosphorus atoms are positioned in the same environment. The ^1H -NMR spectrum of **3** exhibits a doublet at $\delta 1.89$ for the methyl groups on the phosphine ligands due to a coupling ($J_{\text{PH}} = 9.8\text{ Hz}$) to the phosphorus atom. The ^{13}C -NMR spectrum of the C_{60} region at the low temperature (233 K) shows 18 resonances including two signals ($\delta 145.7$ and 144.3 denoted as ●) with double intensity as shown in Fig. 1. This observation indicates the idealized C_3 symmetric nature of **3** in solution, which contains 20 resonances of an equal intensity for the C_{60} moiety, i.e. three atoms of each sp^3 carbon (two types; a and a') and three atoms of each sp^2 carbon (18 types; b ~ l'). The ^{13}C -NMR resonances of the C_{60} ligand for metallofullerenes are typically in the regions of $\delta 175\text{--}135$ for sp^2 carbon atoms and $\delta 85\text{--}50$ for sp^3 carbon atoms [1b]. The two unique high-field resonances of **3** at $\delta 61.8$ and 55.3 are assigned to the sp^3 carbon atoms (a and a') bonded directly to the metal atoms, and are comparable to the resonances of the sp^3 carbon atoms in $\text{Os}_3(\text{CO})_9(\mu_3\text{-}\eta^2, \eta^2, \eta^2\text{-C}_{60})$ ($\delta 61.2$) and **1** ($\delta 57.2, 57.1, \text{ and } 56.7$) [6]. In $\eta^2\text{-C}_{60}$ complexes, the sp^2 carbon atoms adjacent to the sp^3 generally resonate at uniquely low fields above ca. 150 ppm [1b]. If this generality were to hold for the $\mu_3\text{-}\eta^2, \eta^2, \eta^2\text{-C}_{60}$ moiety in **3**, the two lowest-field resonances at $\delta 165.1$ and 158.0 can be assigned to the c and c' carbon atoms.

2.2. Crystal structures of **2**· CS_2 and **3**· $2\text{CH}_2\text{Cl}_2$

The overall molecular geometry and the atomic labeling scheme of **2** and **3** are illustrated in Figs. 2 and 3, respectively. Selected interatomic distances and angles are listed in Tables 1 and 2 for compound **2**, and in Tables 3 and 4 for compound **3**.

Compound **2** has two inequivalent PMe_3 ligands, which are equatorially positioned, at two osmium centers. This is in contrast with the previously reported C_{2v} structures of disubstituted triosmium complexes, $\text{Os}_3(\text{CO})_{10}(\text{PR}_3)_2$ ($\text{R} = \text{Ph}, \text{OCH}_2\text{CF}_3, \text{OMe}$) [9], where the two equatorial phosphine ligands on adjacent osmium atoms are *trans* to each other at the ends of the Os-Os vector. However, a crystal structure analogous to that of **2** has recently been reported for $\text{Os}_3(\text{CO})_{10}(\text{PPh}_3)_2$, in which the two phosphine ligands are *cis* and *trans* with respect to the phosphine-substituted edge [10].

A six-membered carbon ring (C_6 ring) of the C_{60} ligand positions centrally over the Os_3 framework as shown in other reported $\mu_3\text{-}\eta^2, \eta^2, \eta^2\text{-C}_{60}$ complexes. The C_6 ring is parallel essentially with the Os_3 plane with a dihedral angle of 1.3° [cf. 0.9° for $\text{Ru}_3(\text{CO})_9(\mu_3\text{-}$

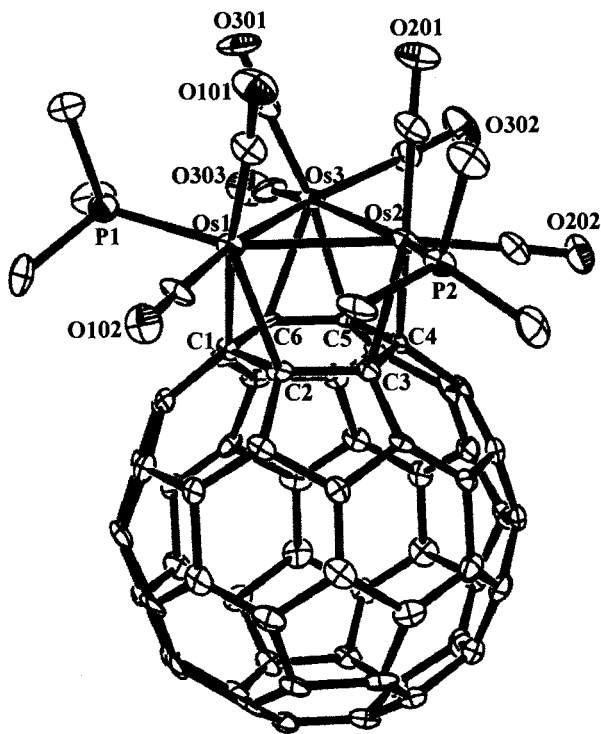


Fig. 2. Molecular geometry and atomic labeling scheme for 2.

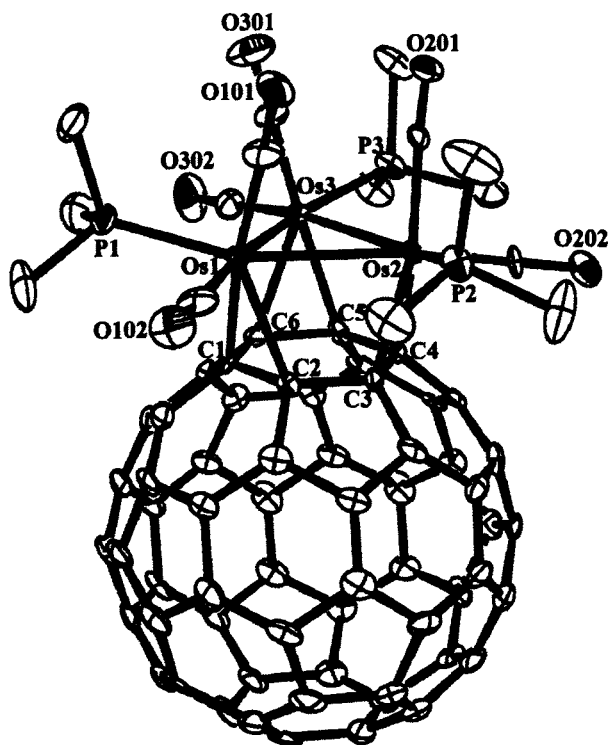


Fig. 3. Molecular geometry and atomic labeling scheme for 3.

$\eta^2, \eta^2, \eta^2\text{-C}_{60}$) [7] and 1.2° for $\text{Os}_3(\text{CO})_8(\text{PPh}_3)(\mu_3\text{-}\eta^2, \eta^2, \eta^2\text{-C}_{60})$ [6]. The two $\text{Os}(\text{CO})_2(\text{PMe}_3)$ and one $\text{Os}(\text{CO})_3$ units are twisted slightly, all in the same direction, so that the three axial carbonyls are disposed in a propeller-like configuration and each pair of equa-

torial ligands is placed one above and one below the Os_3 plane. The bulky phosphine ligands are oriented away from the C_{60} ligands, presumably, due to their unfavorable steric interaction with the C_{60} ligand. The carbon–carbon bonds in the C_6 ring of C_{60} alternate in length (av. 1.48(2) and 1.44(2) Å), and osmium atoms are π -bonded to the short carbon–carbon bonds. Osmium–carbon (C_{60}) bonds also alternate in length (av. 2.29(1) and 2.24(1) Å), resulting in a slight twist of the Os_3 -triangle with respect to the C_6 ring.

The crystal of 3 includes two independent $\text{Os}_3\text{-(CO)}_6(\text{PMe}_3)_3(\mu_3\text{-}\eta^2, \eta^2, \eta^2\text{-C}_{60})$ molecules of mirror images (A and B) and four CH_2Cl_2 solvate molecules in an asymmetric unit. The osmium triangular cores are disordered in both molecules: the osmium triangle in the minor disordered portion is related to that in the major disordered form by a rotation of ca. 54° and a dihedral angle of 4° . This ‘Star-of-David’ type disorder has been reported previously in several triosmium and triruthenium derivatives [11,12].

Compound 3 has a distorted C_3 symmetric nature with three equatorial phosphine ligands, which are arranged as far from the other two as possible, as reported in $\text{Os}_3(\text{CO})_9(\text{PPh}_3)_3$ [11]. The general structural features of 3 are similar to those of 2, adopting an analogous propeller-like configuration of carbonyl and phosphine ligands. The three bulky phosphine ligands are also disposed away from the C_{60} ligand. The planes of the osmium triangle and the C_6 ring of C_{60} are parallel (dihedral angles: 0.4° for molecule A and 0.1° for molecule B). The $\text{Os}\text{-C}(\text{C}_{60})$ bonds alternate in length, (av. 2.28(1), 2.22(1) Å for molecule A and av. 2.29(1), 2.26(1) Å for molecule B). However, the carbon–carbon bonds in the C_6 ring do not show apparent

Table 1
Selected interatomic distances (Å) and estimated S.D.s for 2·CS₂

<i>Metal–metal distances</i>			
Os(1)–Os(2)	2.916(1)	Os(1)–Os(3)	2.960(1)
Os(2)–Os(3)	2.897(1)		
<i>Metal–carbon (carbonyl) distances</i>			
Os(1)–C(101)	1.89(2)	Os(1)–C(102)	1.87(2)
Os(2)–C(201)	1.89(2)	Os(2)–C(202)	1.89(2)
Os(3)–C(301)	1.95(2)	Os(3)–C(303)	1.89(2)
Os(3)–C(302)	1.89(2)		
<i>Metal–phosphorus distances</i>			
Os(1)–P(1)	2.352(5)	Os(2)–P(2)	2.349(4)
<i>Metal–carbon (C₆₀) distances</i>			
Os(1)–C(1)	2.23(1)	Os(1)–C(2)	2.28(1)
Os(2)–C(3)	2.28(1)	Os(2)–C(4)	2.31(1)
Os(3)–C(5)	2.22(1)	Os(3)–C(6)	2.27(1)
<i>Distances within the C₆₀ ligand</i>			
C(1)–C(2)	1.44(2)	C(2)–C(3)	1.49(2)
C(3)–C(4)	1.45(2)	C(4)–C(5)	1.47(2)
C(5)–C(6)	1.43(2)	C(1)–C(6)	1.49(2)

Table 2
Selected interatomic angles (°) and estimated S.D.s for **2**-CS₂

<i>Intermetallic angles</i>			
Os(2)–Os(1)–Os(3)	59.09(2)	Os(1)–Os(2)–Os(3)	61.21(2)
<i>M–M–CO and M–M–P angles</i>			
Os(2)–Os(1)–C(101)	80.4(6)	Os(3)–Os(1)–C(101)	97.8(5)
Os(2)–Os(1)–C(102)	119.8(6)	Os(3)–Os(1)–C(102)	172.2(5)
Os(2)–Os(1)–P(1)	152.4(1)	Os(3)–Os(1)–P(1)	95.1(1)
Os(1)–Os(2)–C(201)	94.5(5)	Os(3)–Os(2)–C(201)	82.1(5)
Os(1)–Os(2)–C(202)	170.7(5)	Os(3)–Os(2)–C(202)	113.1(5)
Os(1)–Os(2)–P(2)	98.0(1)	Os(3)–Os(2)–P(2)	157.7(1)
Os(1)–Os(3)–C(301)	75.8(5)	Os(2)–Os(3)–C(301)	99.6(5)
Os(1)–Os(3)–C(302)	133.6(5)	Os(2)–Os(3)–C(302)	77.8(5)
Os(1)–Os(3)–C(303)	128.4(6)	Os(2)–Os(3)–C(303)	166.9(5)
<i>C–Os–C, and C–Os–P angles</i>			
C(101)–Os(1)–C(102)	89.4(7)	C(201)–Os(2)–C(202)	91.9(7)
C(301)–Os(3)–C(302)	95.4(7)	C(301)–Os(3)–C(303)	92.8(7)
C(302)–Os(3)–C(303)	97.0(8)	C(101)–Os(1)–P(1)	95.0(6)
C(102)–Os(1)–P(1)	87.2(6)	C(201)–Os(2)–P(2)	92.5(5)
C(202)–Os(2)–P(2)	88.6(5)		
<i>Angles involving metal coordinated carbon in C₆₀</i>			
C(2)–C(1)–C(6)	116(1)	C(1)–C(2)–C(3)	124(1)
C(2)–C(3)–C(4)	117(1)	C(3)–C(4)–C(5)	122(1)
C(4)–C(5)–C(6)	119(1)	C(1)–C(6)–C(5)	122(1)

alternation, probably due to the disorder. The average Os–Os distances become longer as carbonyl ligands are substituted with phosphine ligands: 2.877(3) Å for Os₃(CO)₁₂ [13], 2.917(1) Å for Os₃(CO)₈(PPh₃)₃(μ₃-η²,η²,η²-C₆₀) [6], 2.924(1) Å for **2**, and 2.941(1) Å for **3**.

All other features of the molecular geometry of **2** and **3** are within the expected range. The average C–C bond length of the C₆₀ moiety at the junctions of the 5,6 ring and the 6,6 ring are 1.45(2) and 1.38(2) Å for both compounds. The Os–CO distances range from 1.87 to 1.95 Å and from 1.78 to 1.92 Å, C–O bond lengths range from 1.11 to 1.17 Å and from 1.13 to 1.23 Å, and Os–C–O angles are in the range of 174–179° and 171–178° for **2** and **3**, respectively.

2.3. Fluxional behaviors of **1**, **2**, and **3**

The fluxional processes of **1**, **2**, and **3** in solution have been investigated by variable-temperature (VT) ¹³C-NMR spectroscopy using ¹³CO-enriched samples, **1***, **2***, and **3***. Based on the spectroscopic data, compound **1** is assumed to be isomorphous with Os₃(CO)₈(PPh₃)₃(μ₃-η²,η²,η²-C₆₀), in which the phosphine ligand adopts one of the less sterically hindered equatorial positions of the cluster [6]. The ¹³C-NMR spectrum (CO region) of **1*** at 213 K reveals three broad signals at δ 189.1, 181.8, and 178.6 with relative intensities of 1:1:6. The broad signal with an intensity of six may be an overlap of two broad resonances in a 3:3 ratio due to the two inequivalent Os(CO)₃ centers. As the temperature increases to 297 K, the two signals at δ 189.1 and 181.8 coalesce to a single peak (doublet, J_{PC} = 6.2 Hz),

while the broad signal with an intensity of six becomes sharp. Based on this observation, the two low-field and one high-field resonances can be assigned to the two carbonyl ligands on the osmium atom coordinated with PMe₃ and the remaining six carbonyls, respectively. This assignment is consistent with the general trend that carbonyl resonances shift to lower fields as the number of phosphine ligands on metal atoms increases [14]. Furthermore, the lowest field resonance at δ 189.1 can be assigned to the axial carbonyl, based on earlier observations that the resonances of axial carbonyls generally occur at lower fields than those of equatorial carbonyls [4]. The temperature behavior of **1** can be explained by a fast-localized threefold rotation of the three ligands at each osmium center. The phosphine-substituted osmium center may undergo a restricted threefold rotation proposed by Pomeroy and coworkers, without requiring the bulky phosphine ligand to enter an axial site [14]. It is apparent that activation barriers increase as Os(CO)₃ < Os(CO)₂(PMe₃).

The VT ¹³C-NMR spectrum (75 MHz) of **2*** at 213 K (Fig. 4) shows seven resonances at δ 192.9, 191.2, 186.5, 185.3, 184.5, 183.8, and 170.5 with equal intensities.

Table 3
Selected interatomic distances (Å) and estimated S.D.s for **3**·2CH₂Cl₂

	Molecule A	Molecule B
<i>Metal–metal distances</i>		
Os(1)–Os(2)	2.934(1)	2.944(1)
Os(1)–Os(3)	2.947(1)	2.949(1)
Os(2)–Os(3)	2.942(1)	2.927(1)
<i>Metal–carbon (carbonyl) distances</i>		
Os(1)–C(101)	1.89(2)	1.87(2)
Os(1)–C(102)	1.88(2)	1.83(2)
Os(2)–C(201)	1.91(2)	1.91(2)
Os(2)–C(202)	1.78(1)	1.84(2)
Os(3)–C(301)	1.85(2)	1.92(2)
Os(3)–C(302)	1.88(2)	1.83(2)
<i>Metal–phosphorus distances</i>		
Os(1)–P(1)	2.344(4)	2.336(5)
Os(2)–P(2)	2.353(4)	2.336(4)
Os(3)–P(3)	2.343(4)	2.354(5)
<i>Metal–carbon (C₆₀) distances</i>		
Os(1)–C(1)	2.23(1)	2.27(2)
Os(1)–C(2)	2.29(1)	2.30(1)
Os(2)–C(3)	2.22(1)	2.25(1)
Os(2)–C(4)	2.27(1)	2.31(1)
Os(3)–C(5)	2.21(1)	2.25(1)
Os(3)–C(6)	2.28(1)	2.27(2)
<i>Distances within the C₆₀ ligand</i>		
C(1)–C(2)	1.46(2)	1.46(2)
C(2)–C(3)	1.46(2)	1.47(2)
C(3)–C(4)	1.50(2)	1.47(2)
C(4)–C(5)	1.47(2)	1.48(2)
C(5)–C(6)	1.50(2)	1.40(2)
C(1)–C(6)	1.46(2)	1.53(2)

Table 4
Selected interatomic angles (°) and estimated S.D.s for 3·2CH₂Cl₂

	Molecule A	Molecule B
<i>Intermetallic angles</i>		
Os(2)–Os(1)–Os(3)	60.04(2)	59.56(2)
Os(1)–Os(2)–Os(3)	60.21(2)	60.30(2)
<i>M–M–CO and M–M–P angles</i>		
Os(2)–Os(1)–C(101)	79.6(5)	79.3(5)
Os(3)–Os(1)–C(101)	93.3(5)	96.3(5)
Os(2)–Os(1)–C(102)	118.3(5)	117.9(6)
Os(3)–Os(1)–C(102)	172.7(5)	172.8(5)
Os(2)–Os(1)–P(1)	153.4(1)	153.0(1)
Os(3)–Os(1)–P(1)	95.4(1)	95.7(1)
Os(1)–Os(2)–C(201)	94.4(4)	93.5(6)
Os(3)–Os(2)–C(201)	79.1(4)	78.7(6)
Os(1)–Os(2)–C(202)	172.1(5)	173.5(6)
Os(3)–Os(2)–C(202)	117.9(5)	115.4(5)
Os(1)–Os(2)–P(2)	95.1(1)	97.6(1)
Os(3)–Os(2)–P(2)	153.0(1)	155.8(1)
Os(1)–Os(3)–C(301)	80.5(6)	80.0(6)
Os(2)–Os(3)–C(301)	96.6(5)	95.9(5)
Os(1)–Os(3)–C(302)	118.9(5)	116.7(7)
Os(2)–Os(3)–C(302)	172.4(5)	171.6(6)
Os(1)–Os(3)–P(3)	152.5(1)	153.9(1)
Os(2)–Os(3)–P(3)	95.0(1)	95.9(1)
<i>C–Os–C, and C–Os–P angles</i>		
C(101)–Os(1)–C(102)	93.3(7)	89.6(7)
C(101)–Os(1)–P(1)	92.9(5)	94.0(5)
C(102)–Os(1)–P(1)	87.4(5)	87.9(6)
C(201)–Os(2)–C(202)	92.7(6)	90.2(8)
C(201)–Os(2)–P(2)	93.0(4)	94.1(6)
C(202)–Os(2)–P(2)	88.0(5)	87.5(5)
C(301)–Os(3)–C(302)	90.4(7)	91.0(7)
C(301)–Os(3)–P(3)	92.8(6)	93.8(7)
C(302)–Os(3)–P(3)	87.6(5)	88.5(7)
<i>[3]Angles involving metal coordinated carbon in C₆₀</i>		
C(2)–C(1)–C(6)	120(1)	117(1)
C(1)–C(2)–C(3)	121(1)	122(1)
C(2)–C(3)–C(4)	119(1)	120(1)
C(3)–C(4)–C(5)	121(1)	119(1)
C(4)–C(5)–C(6)	119(1)	123(1)
C(1)–C(6)–C(5)	121(1)	120(1)

ties and is consistent with the molecular structure observed in the solid state. Interestingly, compound **2** exists as one isomer in solution, in contrast to the disubstituted derivatives, Os₃(CO)₁₀(PPh₃)₂, where different structural isomers are in a rapid equilibrium [10]. Increasing the temperature causes the three broad resonances at δ 186.5, 184.5, and 170.5 to broaden and become a sharp single peak at 373 K. These three broad resonances are assigned to the carbonyls on the unique Os(CO)₃ center, which undergoes a fast localized three-fold rotation. At higher temperatures, the remaining four resonances due to four carbonyls on the two Os(CO)₂(PMe₃) center start to broaden at similar rates, coalesce, and merge into two distinct peaks (δ 187.4 and 187.3) at 373 K. The two carbonyls on each

Os(CO)₂(PMe₃) are diastereotopic and thus cannot be equilibrated by any threefold rotation process at each osmium center. However, it is probable that coupled restricted rotation at each Os(CO)₂(PMe₃) center would serve to equilibrate the two enantiomers of **2** as shown in Scheme 1. This is implied by the ³¹P-NMR of **2** that reveals two resonances at δ –41.3 and –49.0 of an equal intensity at 213 K, and at high temperatures a typical exchange behavior of the two resonances. The coupled restricted rotation mechanism could lead to equilibrate an axial carbonyl on the osmium center with an equatorial carbonyl on the other, and vice versa (a ↔ d and b ↔ c). If the four lines (δ 192.9, 191.2, 185.3 and 183.8) observed at low temperature exchanged pairwise such as δ 192.9 with 183.8 and 191.2 with 185.3, this could lead to two peaks that are closely spaced at around δ 187, observed at high temperature. This pattern of exchange was proved by obtaining ¹³C-NMR spectrum of **2*** at 393 K on a higher field (100 MHz)

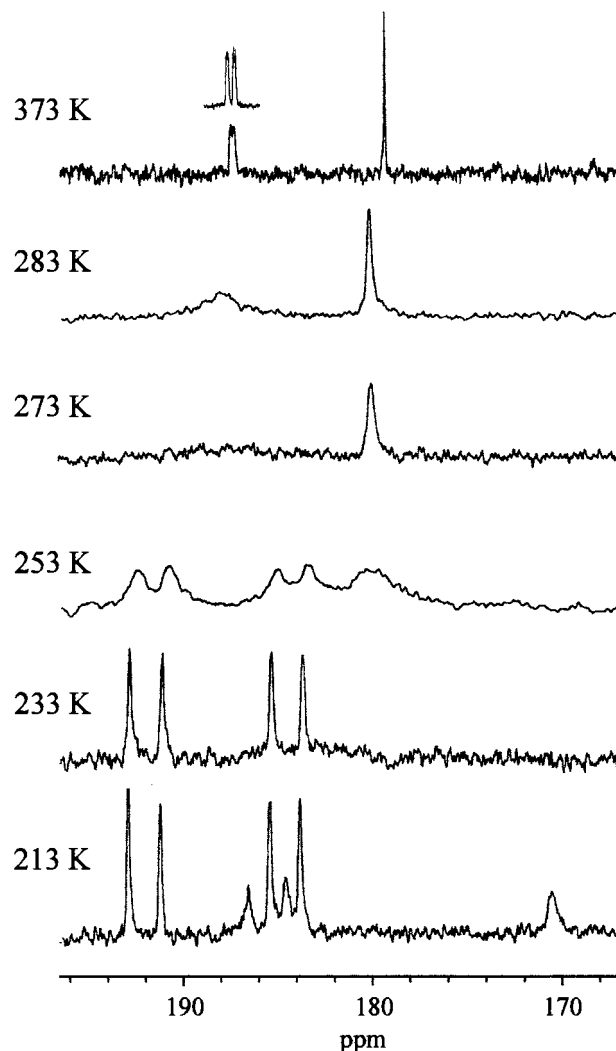


Fig. 4. VT ¹³C-NMR spectra (75 MHz, *o*-C₆H₄Cl₂-C₇D₈, carbonyl region) of **2***. The inset is resonances due to (a, d) and (b, c) carbonyls at 393 K (100 MHz, *o*-C₆H₄Cl₂-C₇D₈).

Coupled restricted rotation mechanism

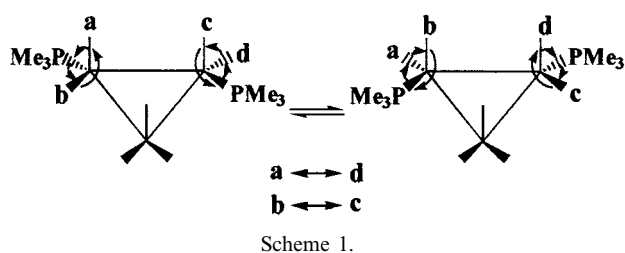


Table 5
 $\Delta G_{\ddagger}^{\ddagger}$ values for the fluxional processes on the $\text{Os}(\text{CO})_2(\text{PMe}_3)_2$ centers

Compound	$\Delta G_{\ddagger}^{\ddagger}$ (kcal mol ⁻¹)	T_c (K)	Resonances employed
1	11.2 ± 0.3	253 ± 5	δ 189.1 and 181.8 in ¹³ C-NMR
2	12.3 ± 0.3	283 ± 5	δ -41.3 and -49.0 in ³¹ P-NMR
3	14.9 ± 0.2	333 ± 5	δ 195.1 and 188.0 in ¹³ C-NMR

spectrometer (see the inset in Fig. 4), which exhibits a broad peak and a doublet ($J_{\text{PC}} = 7.2$ Hz) for the (a, d) and (b, c) carbonyls.

The ¹³C-NMR spectrum of **3*** at 233 K exhibits two resonances at δ 195.1 and 188.0 with an equal intensity, which can be assigned to the three axial and three equatorial carbonyl ligands, respectively. The two signals broaden at higher temperatures and coalesce at 333 K, which also implies a restricted ligand rotation on each osmium center.

The free-energy activation values ($\Delta G_{\ddagger}^{\ddagger}$) of the fluxional processes for the phosphine-substituted centers were calculated from the coalescence temperature and peak separation of the two resonances employed using the Eyring equation [15]. The results for compounds **1**, **2**, and **3** are summarized in Table 5: $\Delta G_{\ddagger}^{\ddagger}$ values increase according to the degree of phosphine substitution. The well-known, pairwise terminal-bridge carbonyl exchange process has been proposed in the clusters $\text{Os}_3(\text{CO})_{12-n}[\text{P}(\text{OMe})_3]_n$ ($n = 2-4$) [14]. The activation barriers for the carbonyl exchange of these complexes are reported to decrease due to the electronic donor effect as substitution of a carbonyl ligand by phosphorus donor ligand increases. However, this terminal-bridge carbonyl exchange process occurring in a plane perpendicular to the Os_3 plane is precluded in complexes **1-3** due to the axially substituted $\mu_3\text{-}\eta^2, \eta^2, \eta^2\text{-C}_{60}$ ligand. Therefore, activation barriers for the restricted threefold ligand rotation of these complexes increase with increasing phosphine substitution, presumably, due to the steric effect of the phosphine ligands.

3. Experimental

3.1. General comments

All reactions were carried out under a nitrogen atmosphere with the use of standard Schlenk techniques. Solvents were dried appropriately before use. C_{60} (99.5%, Southern Chemical Group) and trimethylphosphine (97%, Aldrich) were used without further purification. Anhydrous trimethylamine N-oxide (m.p. 225–230°C) was obtained from $\text{Me}_3\text{NO}\cdot 2\text{H}_2\text{O}$ (98%, Aldrich) by sublimation (three times) at 90–100°C under vacuum. $\text{Os}_3(\text{CO})_9(\mu_3\text{-}\eta^2, \eta^2, \eta^2\text{-C}_{60})$, $\text{Os}_3(\text{CO})_8(\text{PMe}_3)(\mu_3\text{-}\eta^2, \eta^2, \eta^2\text{-C}_{60})$ (**1**), and $\text{Os}_3(\text{CO})_7(\text{PMe}_3)_2(\mu_3\text{-}\eta^2, \eta^2, \eta^2\text{-C}_{60})$ (**2**) were prepared according to the literature methods [5,6]. ¹³C (*C) CO-enriched complexes **1*–3***, were prepared by using $\text{Os}_3(^*\text{CO})_{12}$ (ca. 35% enrichment) [14]. Preparative thin-layer chromatography (TLC) plates were prepared with silica gel GF₂₅₄ (type 60, E. Merck).

Infrared spectra were obtained on a Bruker Equinox-55 FT-IR spectrophotometer. ¹H (300 MHz), ¹³C (75 or 100 MHz), and ³¹P (122 MHz)-NMR spectra were recorded on either a Bruker AM-300 or an Avance-400 spectrometer. Positive-ion FAB mass spectra (FAB⁺) were obtained by the staff of the Korea Basic Science Center, and all m/z values were referenced to ¹⁹²Os. Elemental analyses were provided by the staff of the Agency for Defense Development.

3.2. ¹³C (carbonyl region) and ³¹P-NMR data of **1** and **2**

Compound **1**: ¹³C{¹H}-NMR (*o*-C₆H₄Cl₂-C₇D₈) δ 189.1 (s, br, 1CO), 181.8 (s, br, 1CO), 178.6 (s, br, 6CO) at 213 K; δ 185.1 (d, ² $J_{\text{PC}} = 6.2$ Hz, 2CO), 178.2 (s, 6CO) at 297 K. ³¹P{¹H}-NMR (CS₂-C₆D₆) δ -47.4 (s) at 297 K. Compound **2**: ¹³C{¹H}-NMR (*o*-C₆H₄Cl₂-C₇D₈) δ 192.9 (s, 1CO), 191.2 (s, 1CO), 186.5 (s, br, 1CO), 185.3 (s, 1CO), 184.5 (s, br, 1CO), 183.8 (s, 1CO), 170.5 (s, br, 1CO) at 213 K; δ 187.4 (s, 2CO), 187.3 (s, 2CO), 179.3 (s, 3CO) at 373 K. ³¹P{¹H}-NMR (*o*-C₆H₄Cl₂-C₇D₈) δ -41.3 (s), -49.0 (s) at 213 K; δ -47.1 (s) at 297 K.

3.3. Preparation of $\text{Os}_3(\text{CO})_6(\text{PMe}_3)_3(\mu_3\text{-}\eta^2, \eta^2, \eta^2\text{-C}_{60})$ (**3**)

A chlorobenzene (15 ml) solution of $\text{Os}_3(\text{CO})_9(\mu_3\text{-}\eta^2, \eta^2, \eta^2\text{-C}_{60})$ (30.0 mg, 0.0194 mmol) and PMe_3 (0.01 ml, 0.1 mmol) was prepared in a 100 ml Schlenk flask which was connected to a bubbler. The solution was cooled to 0°C, and Me_3NO (4.4 mg, 0.059 mmol, three equivalents) in 5 ml acetonitrile was added dropwise. The reaction mixture was stirred at 0°C for 30 min, and then heated at 70°C for 1 h. Evaporation of solvents

Table 6
Crystallographic data for **2**·CS₂ and **3**·2CH₂Cl₂

	2 ·CS ₂	3 ·2CH ₂ Cl ₂
Formula	C ₇₃ H ₁₈ O ₇ P ₂ Os ₃ ·CS ₂	C ₇₅ H ₂₇ O ₆ P ₃ Os ₃ ·2CH ₂ Cl ₂
Formula weight	1715.54	1857.33
Crystal system	Triclinic	Monoclinic
Space group	<i>P</i> $\bar{1}$	<i>P</i> 2 ₁ / <i>c</i>
<i>a</i> (Å)	9.9577(5)	26.7007(5)
<i>b</i> (Å)	14.6125(7)	13.1288(3)
<i>c</i> (Å)	17.3557(9)	32.5947(7)
α (°)	97.142(1)	90
β (°)	90.457(1)	90.200(0)
γ (°)	95.578(1)	90
<i>V</i> (Å ³)	2493.4(2)	11425.9(4)
<i>Z</i>	2	8
$\rho_{\text{calc.}}$ (g cm ⁻³)	2.285	2.159
Temperature (K)	293(2)	293(2)
Crystal size (mm)	0.39 × 0.22 × 0.21	0.21 × 1.51 × 0.09
λ (Mo–K α) (Å)	0.71073	0.71073
μ (mm ⁻¹)	7.843	6.991
Reflections measured	10 200	46 590
Unique reflections	6681	15 898
Reflections ($F_o > 4\sigma(F_o)$)	5597	11 999
R_1^a	0.0654	0.0651
wR_2^b	0.1684	0.1482
Goodness-of-Fit ^c	1.061	1.057

^a $R_1 = \Sigma||F_o| - |F_c|| / \Sigma|F_o|$.

^b $wR_2 = \{\Sigma[w(F_o^2 - F_c^2)^2] / \Sigma[w(F_o^2)^2]\}^{1/2}$.

^c GOF = $\Sigma[w(F_o^2 - F_c^2)^2] / (\text{no. reflections} - \text{no. parameters})^{1/2}$.

and purification by preparative TLC (CS₂) provided compound **2** (2.7 mg, 0.002 mmol, 9%, $R_f = 0.23$) and compound **3** (18.1 mg, 0.011 mmol, 55%, $R_f = 0.17$) as black solids. IR (CS₂) $\nu(\text{CO})$ 2040 (w), 2000 (vs), 1965 (vs), 1935 (m), 1911 (m) cm⁻¹. ¹H-NMR (CDCl₃, 298 K) δ 1.89 (d, ²J_{PH} = 9.8 Hz). ¹³C{¹H}-NMR (*o*-C₆H₄Cl₂-C₇D₈, CO region) δ 195.1 (s, 3CO), 188.0 (s, 3CO) at 233 K; δ 190.8 (s, br, 6CO) at 373 K. ¹³C{¹H}-NMR (*o*-C₆H₄Cl₂-C₇D₈, 233 K, C₆₀ region) δ 165.1 (3C), 158.0 (3C), 155.0 (3C), 148.6 (3C), 148.0 (3C), 146.4 (3C), 145.9 (3C), 145.7 (6C), 145.1 (3C), 144.9 (3C), 144.7 (3C), 144.3 (6C), 143.3 (3C), 143.3 (3C), 142.8 (3C), 141.3 (3C), 61.8 (3C, sp³ carbon), 55.3 (3C, sp³ carbon). ³¹P{¹H}-NMR (CDCl₃, 298 K) δ -54.3(s). MS (FAB⁺) *m/z* 1692 [M⁺]. Anal. Calc. for C_{75.5}H₂₇O₆P₃SO₃ (**3**·0.5CS₂): C, 52.6; H, 1.58; S, 1.86. Found: C, 52.9; H, 1.34; S, 1.56%.

3.4. X-ray data collection and structure determination of **2**·CS₂ and **3**·2CH₂Cl₂

Crystals of **2** and **3** suitable for X-ray diffraction studies were grown by slow recrystallization at room temperature from a carbon disulfide solution of **2** and a dichloromethane solution of **3**. Brown crystals of **2** (0.39 × 0.22 × 0.21 mm³) and **3** (0.21 × 1.51 × 0.09

mm³) were mounted on a Siemens SMART diffractometer. Data were collected at room temperature over 14 and 13 h for **2** and **3**, respectively. Preliminary orientation matrix and cell constants were determined with a set of 20 data frames with 30 s collection per frame, followed by spot integration and least-squares refinement. A hemisphere of data was collected using 0.3° ω scans at 30 s per frame. The raw data were integrated (XY spot spread = 1.60, Z spot spread = 0.6) and the unit cell parameters were refined using SAINT [16]. Data analyses and absorption corrections were performed by using Siemens XPREP [17]. The data were corrected for Lorentz and polarization effects, but no correction for crystal decay was applied. Details of relevant crystallographic data are summarized in Table 6.

The structures of **2** and **3** were solved by direct and difference Fourier methods, and were refined by the full-matrix least-squares methods based on F^2 . Hydrogen atoms were not included in the final structure factor calculations. All non-hydrogen atoms were refined with anisotropic thermal coefficients. For all computation, the SHELX97 package was used [18], and function minimized was $\Sigma w(|F_o| - |F_c|)^2$, with $w = 1/[\sigma^2(F_o^2) + (0.1123P)^2]$, where $P = (F_o^2 + 2F_c^2)/3$. For **2**, the number of parameters refined was 793, and the final reliability factors for 5597 unique observed reflections [$F_o > 4\sigma(F_o)$] were $R_1 = 0.0654$, $wR_2 = 0.1684$, with $(\Delta/\sigma)_{\text{max}} = 0.000$, $\Delta\rho_{\text{max}}/\Delta\rho_{\text{min}} = 2.865/-2.766$ e Å⁻³ in the final $\Delta\rho$ map and $S = 1.061$. For **3**, there were two molecules (A and B) in an asymmetric unit, and their geometries were similar. The triangular osmium carbonyl portion in each molecule was disordered in two orientations. However, the carbonyls of minor disordered component could not be located due to their low intensities. All osmium atoms were refined anisotropically, and their occupancies were allowed to vary. The refinement was converged to the following occupancy values: for molecule A, 0.93 and 0.07; for molecule B, 0.87 and 0.13. The number of parameters refined was 1732, and the final reliability factors for 11 999 unique observed reflections [$F_o > 4\sigma(F_o)$] were $R_1 = 0.0651$, $wR_2 = 0.1482$, with $(\Delta/\sigma)_{\text{max}} = 0.001$, $\Delta\rho_{\text{max}}/\Delta\rho_{\text{min}} = 3.591/-1.906$ e Å⁻³ in the final $\Delta\rho$ map and $S = 1.057$.

4. Supplementary material

Crystallographic data for the structures of **2** and **3** have been deposited with the Cambridge Crystallographic Data Centre as supplementary publication nos. CCDC-133679 and CCDC-133680, respectively. Copies of the data can be obtained, free of charge, on application to CCDC, 12 Union Road, Cambridge CB2 1EZ, UK (Fax: +44-1223-336033 or e-mail: deposit@ccdc.cam.ac.uk).

Acknowledgements

We are grateful to the Korea Science and Engineering Foundation for financial support of this research (Project no. 1999-1-122-001-5).

References

- [1] (a) A.L. Balch, M.M. Olmstead, *Chem. Rev.* 98 (1998) 2123. (b) A.H.H. Stephens, M.L.H. Green, *Adv. Inorg. Chem.* 44 (1997) 1. (c) J.R. Bowser, *Adv. Organomet. Chem.* 36 (1994) 57.
- [2] (a) P.J. Fagan, J.C. Calabrese, B. Malone, *Science* 252 (1991) 1160. (b) A.L. Balch, J.W. Lee, B.C. Noll, M.M. Olmstead, *Inorg. Chem.* 32 (1993) 3577. (c) R.E. Douthwaite, M.L.H. Green, A.H.H. Stephens, J.F.C. Turner, *J. Chem. Soc. Chem. Commun.* (1993) 1522. (d) H.-F. Hsu, Y. Du, T.E. Albrecht-Schmitt, S.R. Wilson, J.R. Shapley, *Organometallics* 17 (1998) 1756.
- [3] (a) M. Rasinkangas, T.T. Pakkanen, T.A. Pakkanen, M. Ahlgrén, J. Rouvinen, *J. Am. Chem. Soc.* 115 (1993) 4901. (b) I.J. Mavunkal, Y. Chi, S.-M. Peng, G.-H. Lee, *Organometallics* 14 (1995) 4454. (c) A.N. Chernega, M.L.H. Green, J. Haggitt, A.H.H. Stephens, *J. Chem. Soc. Dalton Trans.* (1998) 755.
- [4] J.T. Park, J.-J. Cho, H. Song, *J. Chem. Soc. Chem. Commun.* (1995) 15.
- [5] J.T. Park, H. Song, J.-J. Cho, M.-K. Chung, J.-H. Lee, I.-H. Suh, *Organometallics* 17 (1998) 227.
- [6] H. Song, K. Lee, J.T. Park, M.-G. Choi, *Organometallics* 17 (1998) 4477.
- [7] H.-F. Hsu, J.R. Shapley, *J. Am. Chem. Soc.* 118 (1996) 9192.
- [8] (a) K. Lee, H.-F. Hsu, J.R. Shapley, *Organometallics* 16 (1997) 3876. (b) K. Lee, J.R. Shapley, *Organometallics* 17 (1998) 3020.
- [9] M.I. Bruce, M.J. Liddell, C.A. Hughes, J.M. Patrick, B.W. Skelton, A.H. White, *J. Organomet. Chem.* 347 (1988) 181.
- [10] W.K. Leong, Y. Liu, *J. Organomet. Chem.* 584 (1999) 174.
- [11] M.I. Bruce, M.J. Liddell, O. Shawkataly, C.A. Hughes, B.W. Skelton, A.H. White, *J. Organomet. Chem.* 347 (1988) 207.
- [12] R.F. Alex, F.W.B. Einstein, R.H. Jones, R.K. Pomeroy, *Inorg. Chem.* 26 (1987) 3715.
- [13] M.R. Churchill, B.G. DeBore, *Inorg. Chem.* 16 (1977) 878.
- [14] R.F. Alex, R.K. Pomeroy, *Organometallics* 6 (1987) 2437.
- [15] J. Sandström, *Dynamic NMR Spectroscopy*, Academic Press, London, 1982, p. 96.
- [16] SAINT; SAX Area-Detector Integration Program, Version 4.050, Siemens Analytical Instrumentation, Madison WI, 1995.
- [17] XPREP: part of the SHELXTL, Crystal Structure Determination Package, Version 5.04, Siemens Analytical Instrumentation, Madison WI, 1994.
- [18] G.M. Sheldrick, SHELX97, Program for Crystal Structure Refinement, University of Göttingen, Germany, 1997.